

Distribution Agreement

In presenting this thesis as a partial fulfillment of the requirements for a degree from Emory University, I hereby grant to Emory University and its agents the non-exclusive license to archive, make accessible, and display my thesis in whole or in part in all forms of media, now or hereafter now, including display on the World Wide Web. I understand that I may select some access restrictions as part of the online submission of this thesis. I retain all ownership rights to the copyright of the thesis. I also retain the right to use in future works (such as articles or books) all or part of this thesis.

Xinlin Gao

April 9, 2024

Use of TSAR, Thermal Shift Analysis in R, to Identify
Metabolic Acid Molecules that Interact with HIV-1 Capsid

by

Xinlin Gao

Stefan Sarafianos
Co-Adviser

Gordon Bermans
Co-Adviser

Quantitative Theory and Methods

Stefan Sarafianos
Co-Adviser

Gordon Berman
Co-Adviser

David Gorkin
Committee Member

2024

Use of TSAR, Thermal Shift Analysis in R, to Identify
Metabolic Acid Molecules that Interact with HIV-1 Capsid

By

Xinlin Gao

Stefan Sarafianos

Co-Adviser

Gordon Berman

Co-Adviser

An abstract of
a thesis submitted to the Faculty of Emory College of Arts and Sciences
of Emory University in partial fulfillment
of the requirements of the degree of
Bachelor of Science with Honors

Quantitative Theory and Methods

2024

Abstract

Use of TSAR, Thermal Shift Analysis in R, to Identify Metabolic Acid Molecules that Interact with HIV-1 Capsid

By Xinlin Gao

Thermal shift assay (TSA) is a simple, yet versatile technique used to screen for potential *in vitro* protein–ligand interactions. Here, we report a free, open-source software tool TSAR (Thermal Shift Analysis in R) to expedite and streamline the analysis of thermal shift data. The TSAR package incorporates three dynamic workflows to facilitate the analysis of TSA data derived either from individual experiments or large screens of chemical libraries. The pipelines aim to return publication-ready graphics and processed summary statistics. TSAR offers a dashboard-style graphic user interface (GUI) that enables easy use by non-programmers, simplifying TSA analysis while diversifying visualization. Accompanying the development and demonstration purposes of this software package, we screened two chemical libraries of vitamins and metabolic acids. Our method and data identify molecules interacting with the capsid protein (CA) of human immunodeficiency virus type 1 (HIV-1), where the hexameric CA interacts with numerous acids *in vitro*, many of which host potential biological significance given previous reports and subsequent studies.

Use of TSAR, Thermal Shift Analysis in R, to Identify
Metabolic Acid Molecules that Interact with HIV-1 Capsid

By

Xinlin Gao

Stefan Sarafianos

Co-Adviser

Gordon Berman

Co-Adviser

A thesis submitted to the Faculty of Emory College of Arts and Sciences
of Emory University in partial fulfillment
of the requirements of the degree of
Bachelor of Science with Honors

Quantitative Theory and Methods

2024

Acknowledgements

This research was supported in part by the National Institutes of Health (R01 AI120860, P30 AI050409, U54 AI170855, to SGS; WMM was supported in part by T32 GM135060 and F31 AI174951). The content is solely the responsibility of the authors and does not necessarily represent the official views of the National Institutes of Health. SGS acknowledges funding from the Nahmias-Schinazi Distinguished Chair in Research. For providing essential details in making the package, we would like to acknowledge the book R Packages by Hadley Wickham (O'Reilly) ©2015 Hadley Wickham, ISBN: 978-1-491-91059-7.

Author contributions

Conceptualization, WMM, KAK, and SGS; Methodology & Investigation, XG, WMM, XW, HZ, AE, and ZCL; Resources, WMM, KAK, AE, and ZCL; Visualization, XG and WMM; Writing – Original Draft, XG, WMM and SGS; Writing – Review & Editing, XG, WMM, SGS; Supervision, WMM, KAK, and SGS; Funding Acquisition, WMM, KAK and SGS.

Table of Contents

1.	INTRODUCTION	1
1.1	THEORETICAL BACKGROUND OF TSA.....	2
2.	LITERATURE REVIEW AND HYPOTHESIS	4
2.1	COMPUTATIONAL SIGNIFICANCE	4
2.2	BIOLOGICAL HYPOTHESIS	5
3.	METHODS	7
3.1	DISTRIBUTION AND PACKAGE INFORMATION.....	7
3.2	PACKAGE STRUCTURE	7
3.3	STATISTICS AND ANALYSIS	8
3.3.1	TSAR Algorithms	8
3.3.2	Tm B Algorithm.....	9
3.3.3	Tm D Algorithm	11
3.3.4	TSAR Accuracy	12
3.4	THERMAL SHIFT ASSAY (TSA).....	13
3.5	ENDOGENOUS REVERSE TRANSCRIPTION (ERT) ASSAY	15
3.6	CYTOTOXICITY TESTING	15
4.	BIOLOGICAL DATA	16
4.1	VITAMIN LIBRARY	16
4.2	ORGANIC ACID METABOLITE LIBRARY	18
5.	BIOLOGY DATA DISCUSSION.....	20

5.1	UNDERSTANDING INTERACTIONS WITH FOLIC ACID	20
5.2	INHIBITORY EFFORTS OF GALLIC ACID	21
6.	SUPPLEMENT.....	23
6.1	ABBREVIATIONS	23
6.2	SUPPLEMENTARY GRAPHS	25
7.	REFERENCES	26

Note

This thesis paper is closely related to an already published BioRxiv paper, Use of TSAR, Thermal Shift Analysis in R, to identify Folic Acid as a Molecule that Interacts with HIV-1 Capsid, written by the same authors and contains similar work intending to be published later via peer-reviewed publications. [53]

1. Introduction

The HIV-1 capsid protein (CA) is a structural protein of vital importance to the virus, essential to viral entry, reverse transcription, nuclear import, integration, viral assembly and more. It is common practice to conduct thermal shift assay (TSA) to study the unfolding of protein in select condition. Experiments are assessed by calculating T_m (50% protein unfolding temperature) as the standard metric. TSAR, an abbreviation for Thermal Shift Analysis in R, is an open-source package that allows data analysis of TSA data. The package utilizes both Boltzmann-fit and Derivative-modeling methods depending on user preference. Accompanying the development of TSAR, we performed two library screens of a total of 107 samples.

CA proteins *in vivo* assemble as pentamers or hexamer, forming a ring structure (Figure 1). To study the interactions between ligands and the hexameric ring structure, the experiments utilized CA121, cross-linked CA hexamers with mutations A14C/E45C/W184A/M185A [PDB: 3H47] to induce stable structures throughout experimental conditions [3]. In total, we performed TSA screening of two libraries against CA121 coupled with TSAR successfully identified meaningful interactions *in vitro*, where results were corroborated by that of Protein Thermal Shift™ Software (V1.4, Thermo Fisher Scientific) [3][4]. We further studied ligands showcasing positive results with additional dose-dependence study to determine that such if interactions were significant at 7.5 μM , where the ligands and CA121 protein will be at 1-to-1 concentration ratio.

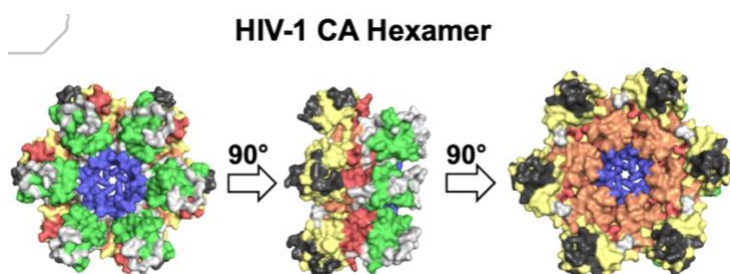


Figure 1. Figure Reproduced from paper, Rotten to the Core, by McFadden WM et al. [18]

1.1 Theoretical Background of TSA

The thermal shift assay (TSA) is an *in vitro* technique quantifying the thermal stability of a purified protein or biological complex as fluorescence measurement over temperature increments in time series [1-3]. During a TSA experiment, samples are heated from below room temperature to boiling temperatures at a constant rate to track the denaturation process of the protein of interest. Utilization of dye is dependent on the structure of protein. Proteins like tryptophan that contain internal aromatic residues can be tracked without a dye while protein such as CA121 used in this protocol require usage of dye like SYPRO™ Orange [4, 5]. The dye's nature of fluorescence in hydrophobic environment of dye allows tracing of hydrophobic residue exposures as denaturation progresses [5]. Plotting fluorescence measurements against the temperature increments gives an individual melting profile for the protein or complex measured. Unless denatured after purification, the fluorescence curve is typically characterized with low initial fluorescence readings and high fluorescence readings near room temperature [7, 8].

The standard thermal profile is sigmoidal, marked with a minimum, steep increase, and plateau at a maximum following by a slow decrease (Figure 2A). A melting temperature (T_m) value can be calculated taking the inflection point of the steep increase or locating the 50% maximum fluorescence using parameter modeling (Figure 2B). T_m values represent the temperature where 50% of the protein is unfolded, useful to compare the thermal stability of proteins under various conditions, such as choosing storage buffers and salts or for comparing the stability of mutant proteins [2, 7, 9, 10]. Since protein-ligand interactions that form additional intramolecular bonds require more energy to denature the sample compared to an unliganded protein, TSA studying of

protein with additional ligands of interest will help inform potential protein-ligand interactions [11, 12].

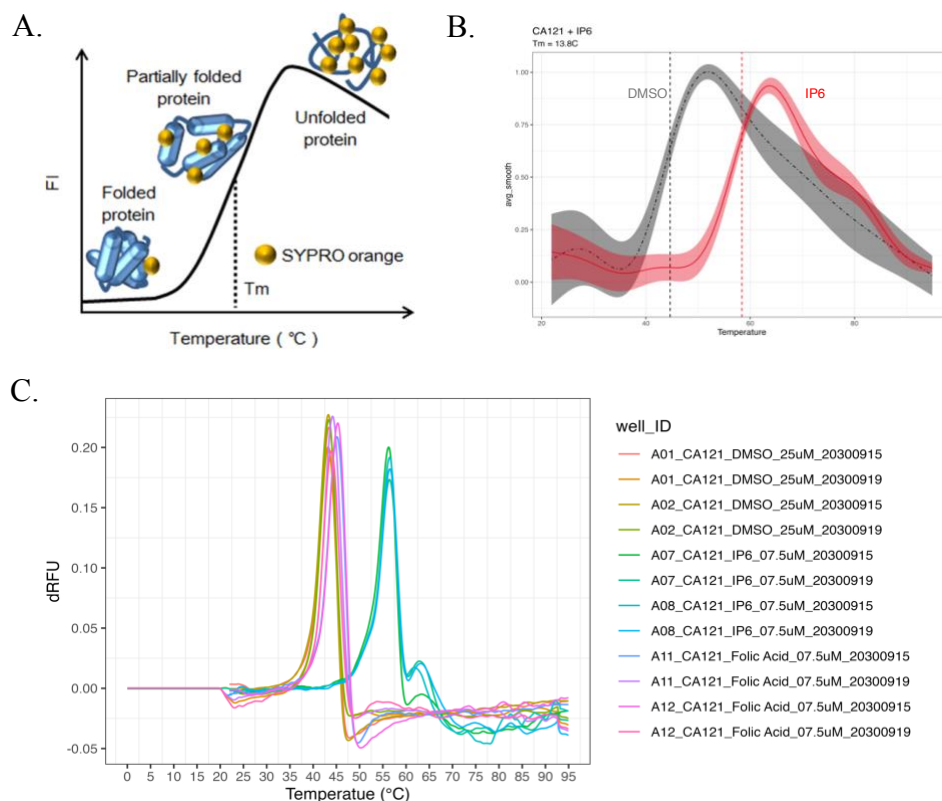


Figure 2. Thermal Shift Assays studies the binding of compounds. A) Figures taken from paper Miyazaki et al [9]. The cartoon figure demonstrates the protein unfolding process where the extent of unfolding is measured by the fluorescence of SYPRO™ orange dye. This protocol focuses on the 50% unfolded state, at which the temperature is recorded as T_m of protein-compound interaction [4,5]. B) Example thermal shift with IP6. Graph is a direct output using the TSAR package. The shifting of curves towards either direction signifies interactions between ligand and protein. Significance is measured as the change in melting temperature (T_m). C) Example first derivative comparison graph comparing results from DMSO, IP6, and Folic Acid under dosage iterations. Comparing the derivatives of fluorescence between conditions captures how significantly one molecule may impact protein unfolding. For example, the IP6 profiles have a common separate small peak trailing the major one.

2. Literature Review and Hypothesis

2.1 Computational Significance

TSA is useful for screening chemical libraries to identify potential binding partners for proteins. It has been used as a proxy readout for *in vitro* ligand binding within screens for protein inhibitors of a specific target given the simplicity of experimental setup.

The current available tools to analyze TSA data include Protein Thermal Shift™ Software v1.4 developed by Thermo Fisher Scientific (Waltham, MA), Serial Explorer implemented in MATLAB, and open-source workflows provided through the Konstanz Information Miner (KNIME) [13]. Although the tools from Thermo Fisher Scientific and MATLAB offer high-throughput analysis capabilities, they are proprietary and entail additional expenses. Despite KNIME being open source, it provides only limited visualization options. In response to the necessity for multidimensional data visualization and improved accessibility of analysis tools, we have developed a software package in R, a programming language extensively utilized for statistical and graphical analysis of biological data.

TSAR, which stands for Thermal Shift Analysis in R, is a software available on Bioconductor and open-source, operating in R (version ≥ 4.3) and distributed under an AGPL-3 license [14, 15] (Figure 3). The TSAR analysis integrates either Boltzmann-fit or derivative-modeling approaches to identify T_m B (Boltzmann-fit) or T_m D (derivative-model) from melting curves, with pipelines facilitating easy comparisons across various dimensions, including T_{ms} , change in T_{ms} (ΔT_m), ligands, dosages, derivatives, and time series.

T_m B, short of Boltzmann equation derived T_m , is a kinetic equation describing the statistical behavior of a system of particles [54]. It is applied widely towards sigmoidal behaviors. Interpreting the Boltzmann equation with respect to energy produces a sigmoidal curve where the curve rises sharply at low energies, reaches a maximum, and then gradually decreases at higher energies. Using parameter-based mathematical modeling, individual melting curves are fit through a 5-parameter [55].

T_m D, standing for derivative-model derived T_m , utilizes smoothing to remove noises from data and produces a polynomial function closely representing the trend and shape of raw data. T_m s are then derived through the calculation of first derivatives and location inflection point [55].

Both methods are used in extant research protocols where T_m B are less affected by trivial fluctuation and T_m D captures all levels of variations throughout the denaturation process. The TSAR package provides a comprehensive set of tools, covering initial data processing, T_m identification, automated data comparisons, and the generation of multiple publication-quality graphics for both individual experiments and large-scale screens with replicates (Figure 3B-E). TSAR is extensively documented and offers numerous customizable settings for proficient R users, while also incorporating wrapping functions and a ShinyR dashboard to streamline usage and facilitate rapid implementation. Overall, TSAR is designed to streamline TSA analysis while enhancing visualization capabilities.

2.2 Biological Hypothesis

HIV-1 capsid protein (CA) holds a crucial role in the macromolecular assembly of mature viral core. The capsid proteins form a ring structure to serve as a reaction chamber for reverse transcription while shielding viral genome from cellular immune sensors during its transit to the

nucleus [16-19]. CA is involved in numerous steps of the HIV-1 replication cycle such as viral entry, reverse transcription, nuclear import, integration, viral assembly and more, making it a hot target of HIV treatment development [17-19]. Given its critical nature, exploring the biology of the capsid core holds significant implications towards the development of next-generation antiretroviral therapies (ART) [18].

CA is a great clinical target, as it is a highly conserved and genetically fragile protein [9, 18]. Furthermore, the kinetics of CA•CA interactions are finely tuned for balancing cellular trafficking and genome release. Such intricacy in structure demands flexibility in protein where either increasing or decreasing capsid stability would negatively impact viral fitness [18, 22-25].

In 2022, Lenacapavir (also called Sunlenca® or GS-6207), the first CA-targeting drug compound, was approved for use in highly-treatment experienced patients, making it the first of its kind. It marked a breakthrough in antiretroviral therapy (ART) as the first new target for a clinically used ART class in over a decade [20, 21].

Recent reports have demonstrated that CA interacts with inositol hexaphosphate (IP6) and deoxyribonucleotides (dNTPs) to stabilize the structure of hexameric ring of capsid protein [26-28]. Furthermore, HIV-1 infected individuals also commonly report modulated cellular metabolism disregard of ART treatment [29, 30]. This observation prompts the hypothesis that there are more endogenous small molecules in cellular metabolism that closely interact with HIV-1 virus.

Thus, using IP6 as the positive control, we screened a library of vitamins (Sigma, St Louis, MO) and a library of endogenous organic acid metabolites (Sigma, St Louis, MO) for interactions with a disulfide-stabilized HIV-1 capsid hexamer, CA121. All data are subsequent processed using the TSAR package to identify potential binding partners to (CA). In summary, we found 20

molecules demonstrating significant ΔT_m shift, leading with Gallic acid, 6.37 °C, Folic acid, 3.04 °C, and Xanthurenic acid, 2.28° (Figures 5 and 8). These screens provide an example workflow for the TSAR R package, a tool that can be broadly used in protein biology.

3. Methods

3.1 Distribution and Package Information

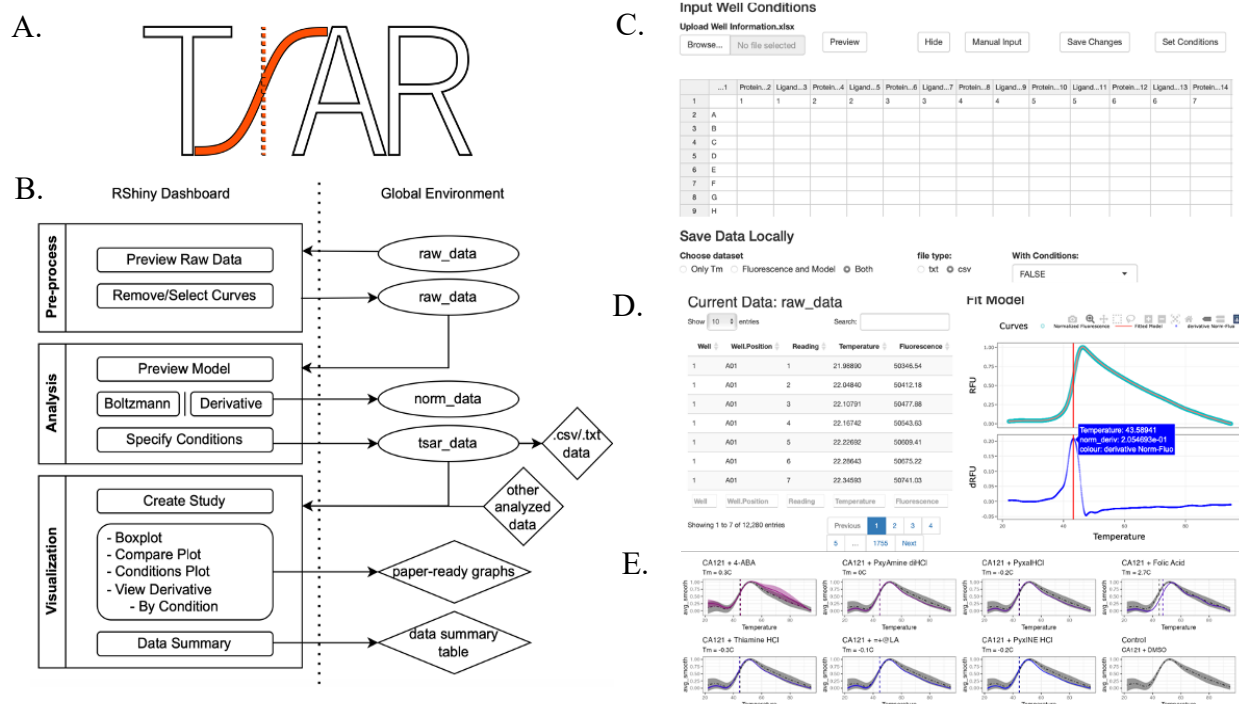
TSAR (Thermal Shift Analysis in R) is an open-source package written in R (≥ 4.3) [15]. It is freely distributed under an AGPL-3 license in the Bioconductor R package repository ($V \geq 3.18$) [31] at <https://bioconductor.org/packages/TSAR>. Downloading TSAR through R requires that the BiocManager R package [32] be installed prior; installing TSAR is accomplished with the following line of code: *BiocManager::install("TSAR")*. TSAR was coded and documented using the RStudio GUI [33] and the devtools package [34]. TSAR contains well-documented functions and three vignettes (long-form documentation) to assist users. TSAR depends on tidyverse packages [35] as well as: jsonlite [36], openxlsx [37], mgcv [38-40], and minpack.lm [41] packages for analysis, and shiny [14], shinyWidgets [42], plotly [43], shinyjs [44], rhandsontable [45], and ggpubr [46] packages for the Shiny R GUI and data visualizations.

3.2 Package Structure

TSAR allows visualization of data on multiple dimensions, taking T_m (50% protein unfolding temperature) analysis further, providing a comparison of numerous dimensions, including aspects of, but not limited to T_m s, ligands, dosages, derivatives, and time series.

To operate, TSAR is sectioned into three individual operating dashboards, Data Preprocessing, Data Analysis, and Data Visualization, each with one command line call (Figure

3B). While users may conduct all procedures and analyses within the established GUI, this package also allows command-line approaches where users may implement more options and flexibilities



with their analysis. Mathematical modeling in TSAR relies on both generalized additive models and non-linear modeling to compute $T_m D$ and $T_m B$ values.

Figure 3. A) TSAR Logo. B) Workflow for TSAR, supporting data import and export at various stages. C-E) Screenshots of the TSAR program. C) shows the Shiny R GUI for importing data. D) shows the interactive data analysis that TSAR performs, E) is an example of a partial output from a library screen.

3.3 Statistics and Analysis

3.3.1 TSAR Algorithms

TSAs result in a standard curve characterized by initial low fluorescence, an increasing peak, and trailing fluorescence slowly decreasing back to the initial level (Figure 2). To study such

peaks, mathematical modeling is required (Figure 2). Combining with machine learning, TSAR utilizes the generalized additive model from the `mgcv` package to capture the derivatives of the curve and the inflection point, $T_m D$ [38-40]. Meanwhile, TSAR utilizes non-linear modeling from the `minpack.lm` package [41] in R to capture Boltzmann curves with machine-learned minimum and maximum. Through such mechanism, TSAR characterizes the fluorescence trend in Boltzmann fit fashion, locating the $T_m B$. Users may switch between both methods easily within the GUI and command line based on preferences of data processing.

3.3.2 $T_m B$ Algorithm

$T_m B$ is derived from the Boltzmann Equation capturing behavior of systems of particles. It is a kinetic equation describing statistical mechanics, often used to study subjects following non-equilibrium [54].

$$\text{Boltzmann Equation:} \quad \frac{\partial f}{\partial t} + v \cdot \nabla f = Q(f) \quad [54, 56]$$

Term f describes the distribution probability density of finding a particle v at a particular position and time. $\frac{\partial f}{\partial t}$ is the rate of change of f with respect to time. $v \cdot \nabla f$ describes the distribution function change of particles moving through space. Lastly, $Q(f)$ is a collision term describing the effects of particles interactions and collisions.

While the Boltzmann Equation does not directly translate to a sigmoidal curve, expanding the equation with respect to energy (E) leads to the following equation.

Boltzmann Distribution:
$$P(E) = \frac{e^{-\frac{E}{kT}}}{Z} \quad [54, 56]$$

$P(E)$ is the probability of finding a particle in an energy state E , which in this case is the measurement of fluorescence. k is the Boltzmann constant. T is the temperature of the system corresponding to the x-axis of TSA data. Lastly, Z is used to normalize functions overall [56]. This sigmoidal shape arises because at low energies, only a few particles have enough energy to occupy higher energy states, while at high energies, the exponential term suppresses the probability [55].

To implement this, TSAR first learns the local minimum and maximum fluorescence to provide a range of modeling. It then calls the minpack.lm package with preset parameter equation to iteratively find the best fitting model. An inflection point or melting temperature (T_m) is then calculated based off of the model.

TSAR Model:
$$y = \frac{1}{1 + e^{-k(x-x^2)}} \quad [56]$$

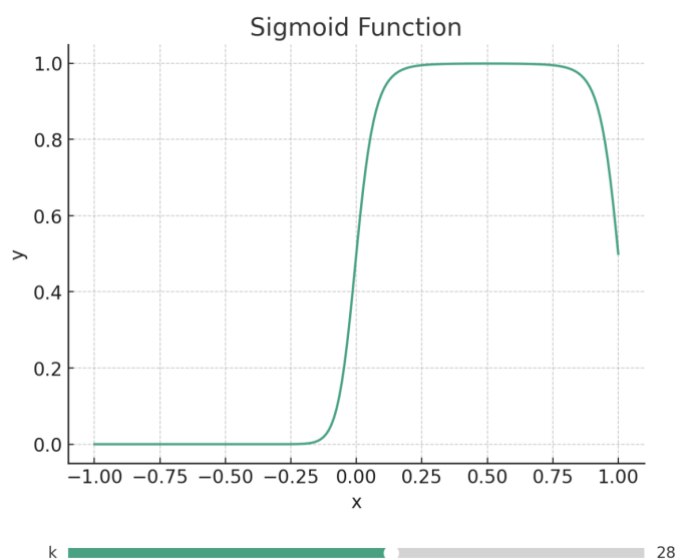


Figure 4. Example TSAR model curve given the formula.

Expressing the model in terms of x as temperature and y as fluorescence, the TSAR package constructed the above equation after training and testing on multiple runs of dataset (Figure 4). The package automatically learns the minimum and maximum temperature using gradient descent algorithms. The fluorescence curve is restricted with the learned threshold temperatures and subsequently fed to fit the above formula by iterating k values to find the best fit model with highest r^2 value.

3.3.3 T_m D Algorithm

T_m D method bases on generalized additive modeling which results in polynomial fitting or formula. Generalized Additive Modeling, GAM, is an extension of traditional linear regression models where multiple randomized models are added to capture non-linear relationships between predictors and response variable. After modeling, a smooth function is used to generate piecewise polynomial functions that best fit all trends observed in raw data.

TSAR package utilizes the gam function from package mgcv. Model assumes 'method = "GACV.Cp"' and sets to 'formula = $y \sim s(x, bs = "ad")$ '. Smoothing may be toggled off by specifying parameters.

The smoothed GAM model is then used to calculate first derivatives and melting temperatures (T_m). This approach is especially accurate in the case of TSA where fluorescent readings following previous readings closely instead of divergent patterns such as flashing. GAM also helps capture nuances of curve such as smaller peaks preceding the major one.

Models and smoothing parameters were selected by sectioning data into training and testing dataset where the smoothing parameter yielding the highest overall fit by, mean r^2 value,

on testing data. Moreover, fitting results of each model of the curve are available for preview and summary data export through the dashboard (Figure 3D).

3.3.4 TSAR Accuracy

To assess the accuracy of TSAR, we benchmarked its calculations of T_m and ΔT_m shift to those of Protein Thermal Shift Software V1.4 (Thermo Fisher Scientific). Setting Protein Thermal Shift Software calculations as the baseline literature value, the error of TSAR T_m D is centered at 0.00 with a variance of 0.11 degree Celsius (Figure 5A). Meanwhile, the error of TSAR T_m B is centered at 1.03 with a variance of 0.63°C (Figure 5B). While that error is relatively greater than T_m D, the error is systematic where computing ΔT_m B by using DMSO as the baseline control yield errors centering at 0.376 °C (Figure 5C-D).

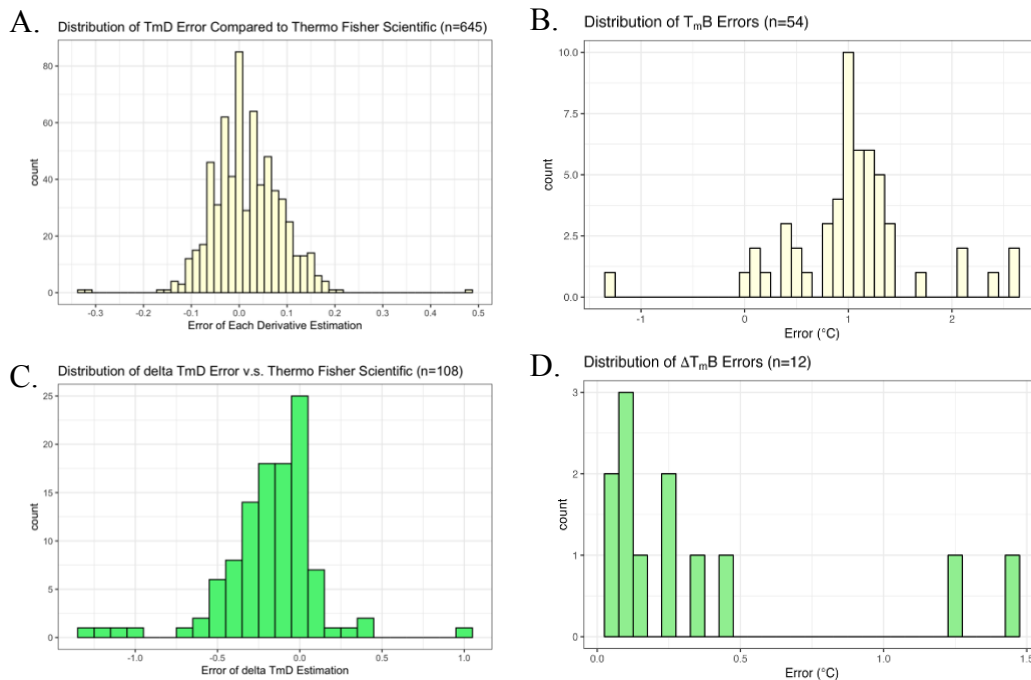


Figure 5. TSAR accuracy compared to Protein Thermal Shift™. A, C) Derivative estimation errors. (n = 645) is $N\sim(0.00, 0.11)$ (normally distributed around mean of 0.00 and standard deviation of 0.11). ΔT_m

D estimation error is similarly distributed, $N(-0.01, 0.03)$. **B, D**) Boltzmann estimation errors ($n = 54$) is approximately $N(-1.03, 0.63)$. ΔT_m B estimation error is biased in the positive direction, centered at 0.38 with a standard deviation of 0.45.

Overall, given the nature of TSA assay application, the focus lies on the accuracy of ΔT_m calculations when compared to the negative control of experiment. Thus, we can conclude, TSAR is effective at determining the significance of a shift.

3.4 Thermal Shift Assay (TSA)

TSAs were conducted using QuantStudio 3 Real-Time PCR Systems (Thermo Fisher Scientific, Waltham, MA) with a final reaction volume of 20 μ L and $\leq 1\%$ DMSO. The sample fluorescence was measured while being heated from 25–95°C at a constant rate of 0.2°C/10 s, consistent with the methodology outlined in previous studies [6, 9, 11]. Proteins were tested at a final concentration of 7.5 μ M in a 50 mM Tris (pH 8.0) and supplemented with 1x SYPRO™ Orange Protein Gel Stain (Life Technologies) after incubation with the compounds for ~30 minutes on ice. In the initial screening of the library, the CA121 protein (7.5 μ M) was incubated with 50 μ M of each compound. Fluorescence intensity for each sample was measured as described, and thermal profiles were assessed using TSAR or Protein Thermal Shift Software v1.3 (Applied Biosystems). The compounds that induced a shift in the T_m (ΔT_m) at 50 μ M underwent further testing in a dose-response manner under concentrations of 7.5 μ M and 25 μ M (Figure 6).

Lastly, all compounds leading to significant thermal shifts were also tested in the presence of the reducing agent tris(2-carboxyethyl) phosphine (TCEP)-treated CA121 or against the wild type full length capsid protein-CA FL. TCEP functions to break the CA121 disulfide stabilizing bonds, possibly affecting the stability of pockets formed by multiple CA monomers [26, 47]. Comparing the fluorescence profile of TSA samples with and without TCEP provides insight into

the potential interactions of a compound with the monomer versus the hexameric CA interface (Figure 6).

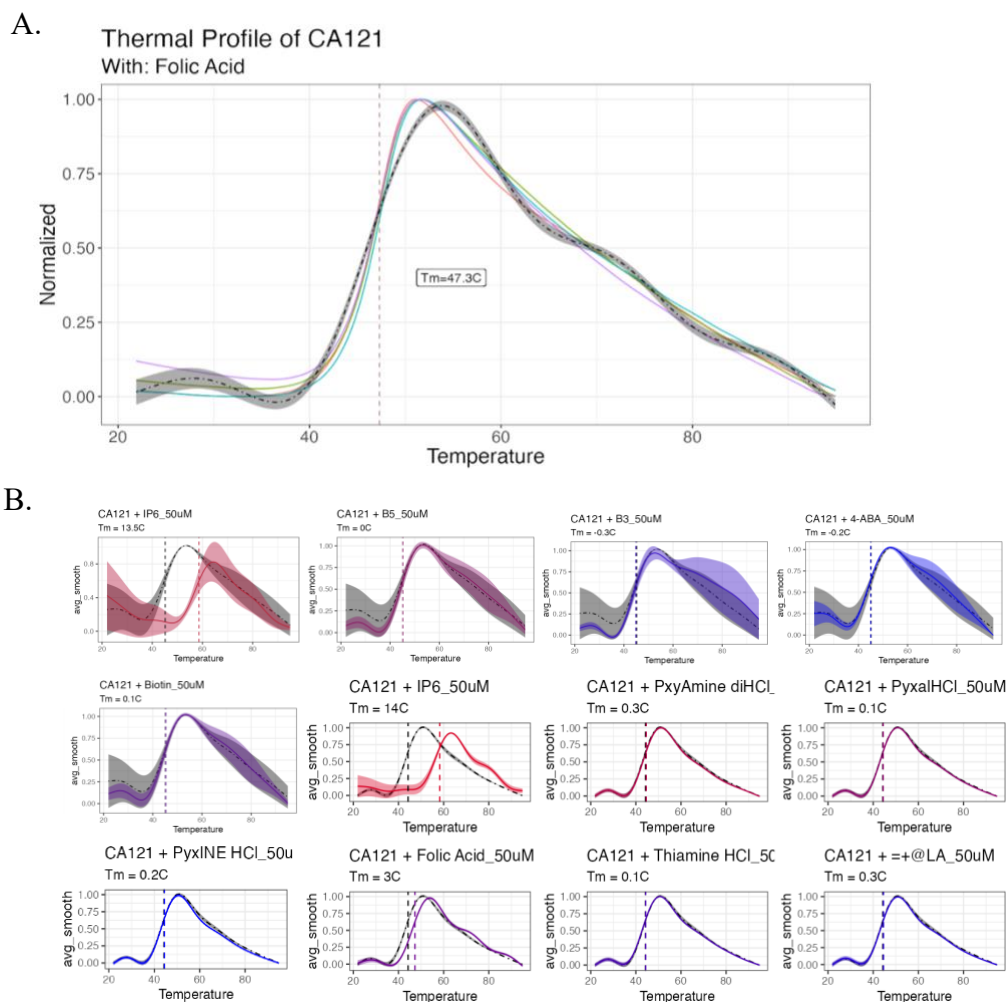


Figure 6. Thermal profiles of the vitamin library showcase significant Folic acid interaction with the CA. Screening all vitamin compounds at 50 μ M with CA121 hexamer protein at 7.5 μ M. All compounds were suspended in DMSO, thus compared to negative control, DMSO. Initial screening shows that folic acid shows a 3.04°C of T_m D shift, indicating interactions with CA121 while it unfolds. **A)** Folic Acid thermal shift assay profiles by individual sample (n = 4). Each individual trial is mapped in a differently colored curve. Graph shows normalized RFU (relative fluorescence unit) as y-axis. Alternate options are allowed in TSAR package. The grey line represents average between all samples of a condition. **B)** Compare

plot further showcases the interaction curves. Graphed as RFU (relative fluorescence unit) over Temperature (°C) in color as contrast to DMSO control in grey. Only IP6, positive control, and Folic Acid yields significant T_m change. IP6: $\Delta T_m D = 13.75^\circ\text{C}$ at significance level $p < 5E-11$. Folic Acid: $\Delta T_m D = 3.04^\circ\text{C}$ at significance level $< 5E-5$.

3.5 Endogenous Reverse Transcription (ERT) Assay

ERT assay determines the expression levels of reverse transcription products within melittin-permeabilized pseudotyped HIV-1 virions (VSV-G-NL4-3 AEn) produced. p24 levels for each virion sample were initially determined by Enzyme-linked immunosorbent assay (ELISA). Subsequently, ERT reactions were conducted using cell supernatants containing pseudotyped virions assembled in the presence of various amounts of BBS-103, which were then normalized to 500 μg of total p24 (both assembled and non-assembled). The reaction mixture included 10 mM Tris-HCl (pH 7.8), 75 mM NaCl, 2 mM MgCl₂, 2.5 $\mu\text{g}/\text{mL}$ melittin, 80 μM IP6, 0.5 mg/mL BSA, and 40 mM dNTPs. Following a 16-hour incubation at 37°C, the products were quantified via qPCR with SYBR green detection, utilizing specific primer sets for the minus-strand strong stop and second-strand transfer, as adapted from the respective sources.

3.6 Cytotoxicity Testing

Assessing compound cytotoxicity involved treating TZM-B1 cells with compounds, followed by the evaluation of cell viability using an XTT kit (Roche) at the conclusion of the treatment period, as per the manufacturer's guidelines. Decreased cell viability, indicating compound-induced toxicity, was determined by normalizing against the viability of DMSO-treated cells. The obtained values were plotted in GraphPad Prism 5 and analyzed using the log (inhibitor) vs. normalized response - variable slope equation to determine the CC_{50} values.

4. Biological Data

4.1 Vitamin Library

Testing the V1-1KT Vitamin kit library from Sigma-Aldrich (Sigma, St Louis, MO) yielded significant result for the folic acid with ΔT_m D shift of 3.04 °C. Testing at 50 μ M, 25 μ M, and 7.5 μ M compound, the first derivative comparison graphs demonstrate that the ΔT_m of folic acid with CA121 is dose dependent (Figure 7). At 7.5 μ M, protein unfolding curves are distinguishable from DMSO control, but ΔT_m experiences greater variance. Conducting one-tailed, paired T tests show that all treatment conditions are significantly different from the DMSO control, with 50 μ M and 25 μ M folic acid significant at the level of 5E-5, and 7.5 μ M folic acid significant at the level of 5E-3 (Figure 8D).

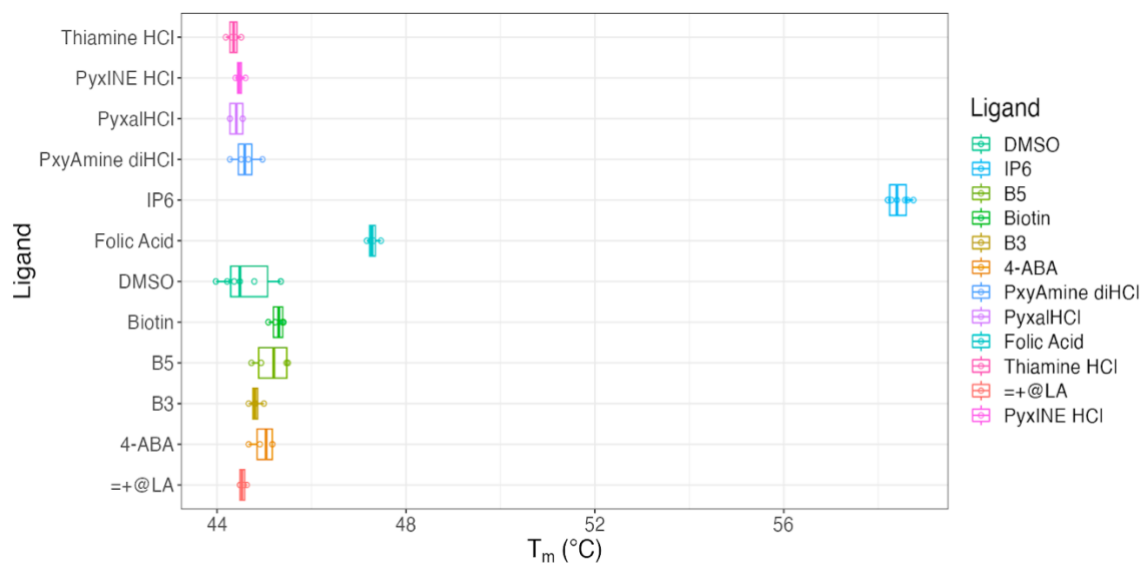


Figure 7. Boxplot of T_m distribution of vitamin library against CA121 hexamer. Screening all vitamin compounds at 50 μM with CA121 hexamer protein at 7.5 μM . All compounds were suspended in DMSO, thus compared to negative control, DMSO. Initial screening shows that folic acid shows a 3.04 $^{\circ}\text{C}$ of T_m D shift, indicating interactions with CA121 while it unfolds. Labels of Ligands follow: a-LA: (\pm)- α -Lipoic acid; 4-ABA: 4-Aminobenzoic acid; B3: Nicotinamide; PyxINE HCl: Pyridoxine hydrochloride; B5: D-Pantothenic acid hemicalcium salt; Thiamin HCl: Thiamine hydrochloride; Pyxal HCl: Pyridoxal hydrochloride; PyxAmine diHCl: Pyridoxamine dihydrochloride

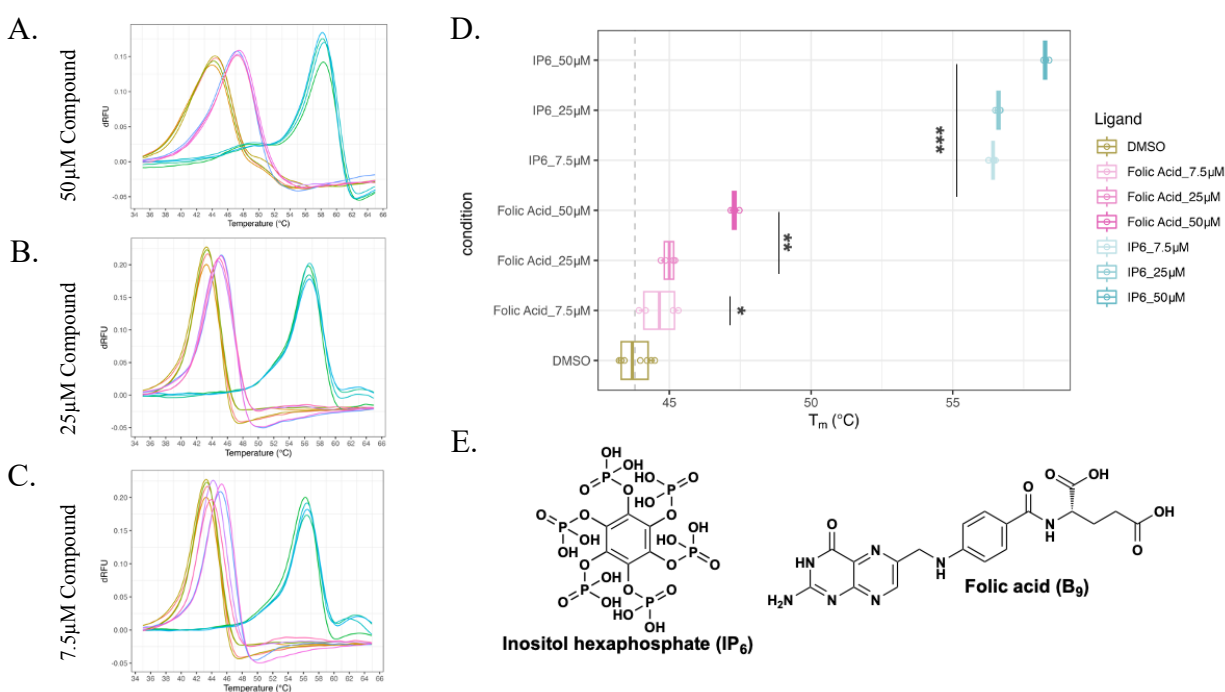


Figure 8. Dose dependence study of folic acid and CA121 shows ΔT_m is dosage-dependent yet still significant. A-C) First derivative comparison graphs demonstrate that ΔT_m of folic acid with CA121 is dose dependent at A) 50 μM , B) 25 μM , C) 7.5 μM compound. At 7.5 μM , protein unfolding curves are distinguishable, but suffers greater variance. D) Each condition (n = 4) consist of ligand suspended in DMSO and CA121 hexamer protein in Tris buffer at pH 8.0. IP6 is diluted in Tris buffer directly without DMSO. One-tailed t-tests show that all treatment conditions are significantly different from the DMSO

control. * indicates significance at 5E-3, ** indicates significance at 5E-5, and *** indicates significance at 5E-9 E) Chemical Structures of hits, Folic Acid and IP6. Made in ChemDraw V19.0.

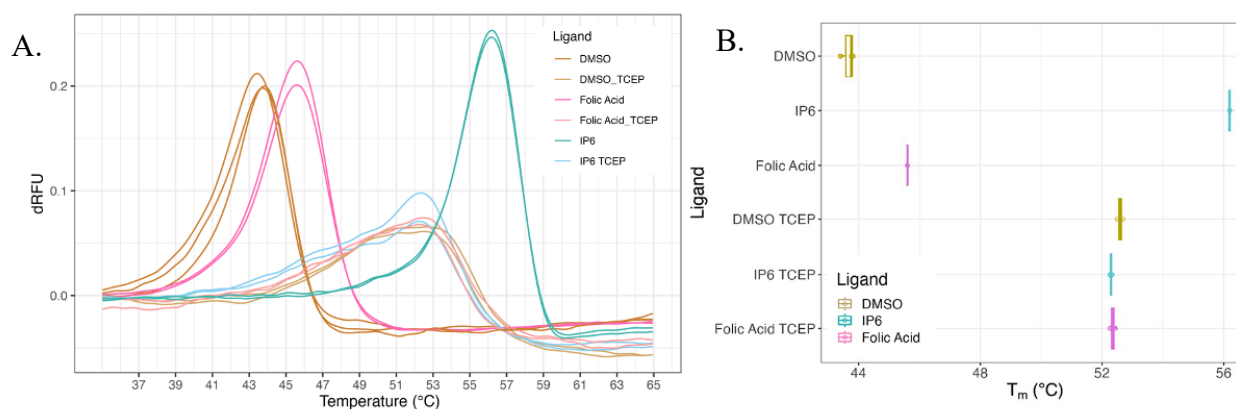


Figure 9. Reducing CA121 shows Thermal Shift in folic acid is protein specific. TCEP was added as a reducing agent to break apart CA121, eliminating the central pore of protein-ligand interaction. A) TSA performed with ligands at 25 μ M. Comparing first derivatives show that TCEP alters regular protein fluorescence curve. B) Boxplot demonstrates adding TCEP leads to insignificant ΔT_m D.

4.2 Organic Acid Metabolite Library

The Organic Acid Metabolite Library from Sigma-Aldrich (Sigma, St Louis, MO) contains 96 samples of endogenous metabolites. All ligands were initially screened at 25 μ M against CA 121 at 7.5 μ M. Each reaction well contained < 1% DMSO, compound, purified CA121, and 50 mM Tris buffer (pH 8.0). Subsequently, ligand hits were tested for dose-dependence at 50 μ M and 7.5 μ M. Ligand screenings have a sample size (n) of 6 each with biological replicates and technical replicates. Following all experiments, thermal shifts of 1°C or greater in either positive or negative directions were considered significant and thus further

studied (Figure 10). Following the highest $\Delta T_m D = 12^\circ\text{C}$ for IP6 is Gallic acid, of which the melting curve shifts in the positive direction with $\Delta T_m D = 6.23^\circ\text{C}$.

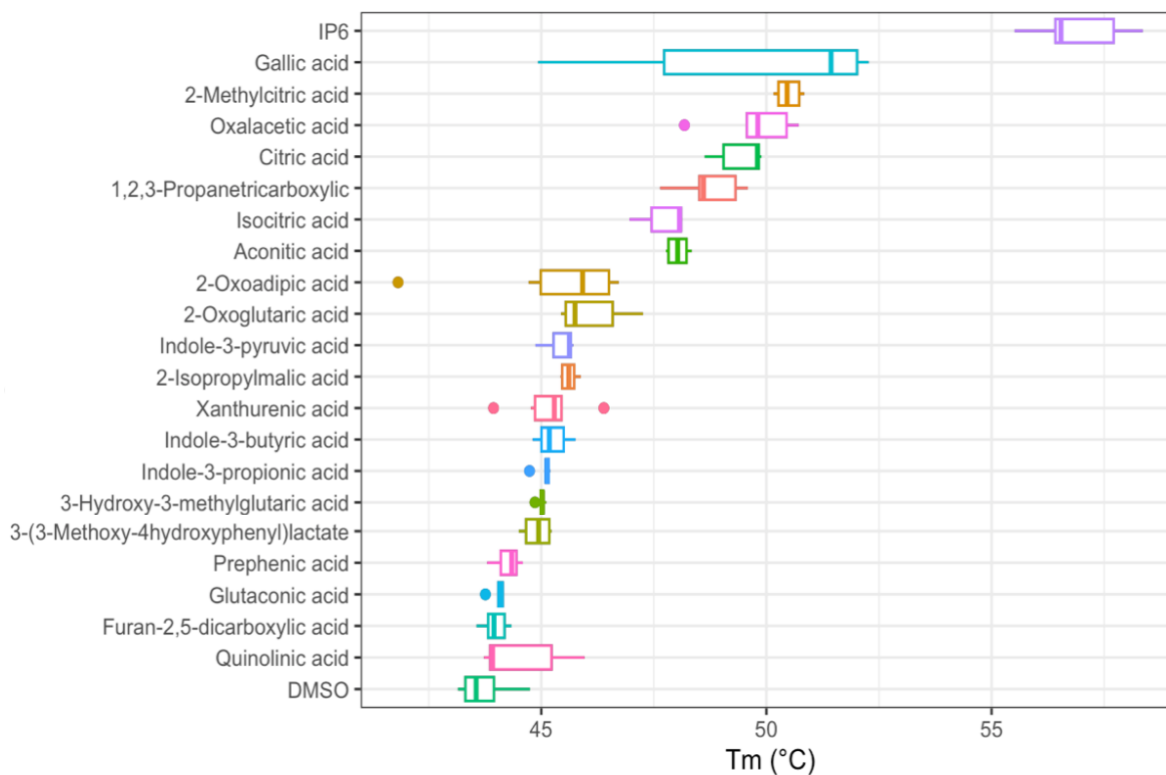


Figure 10. Boxplot of T_m distribution of Metabolic Acid library hits against CA121 hexamer.

Boxplot includes only hits of 96 metabolic acid library where the $\Delta T_m D$ is greater than or equal to 1°C with standard deviation less than 1°C . Screening all metabolic acid compounds at $25\ \mu\text{M}$ with CA121 hexamer protein at $7.5\ \mu\text{M}$. All compounds were suspended in DMSO, thus compared to negative control, DMSO. The metabolic acids library contained 20 hits. Distribution of DMSO T_m is included as a comparison while IP6 is used as a positive control.

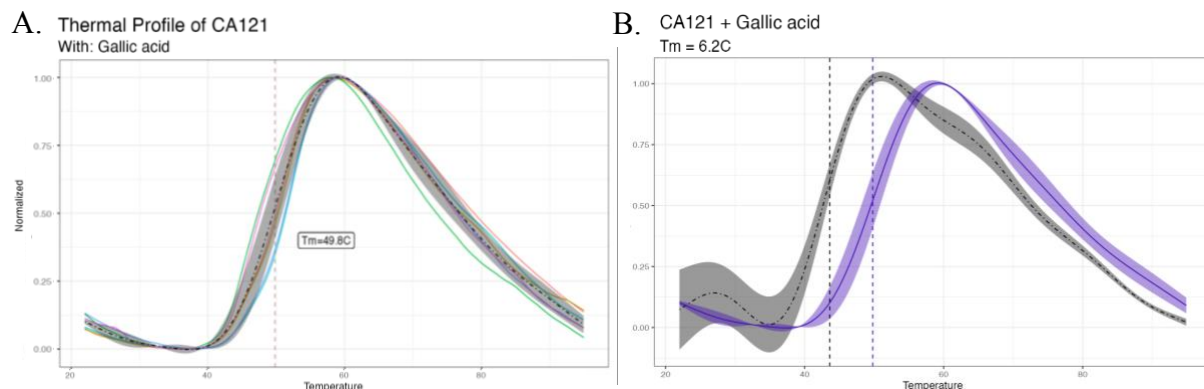


Figure 11. Gallic Acid Profiles and compare plots using DMSO as negative control. a) Gallic Acid ($n = 6$), purple, graphed against DMSO control, grey. Compare plot generated by the graphing dashboard of TSAR, showing 6.23°C of shift when averaged and compared to DMSO. **b)** Gallic Acid thermal shift assay profiles by individual sample ($n = 6$). Each individual trial is mapped in separately colored curve. Graph shows normalized RFU (relative fluorescence unit) as y-axis. Alternate options are allowed in TSAR package. The grey area represents average and standard deviation between all sample.

5. Biology Data Discussion

5.1 Understanding Interactions with Folic Acid

We screened protein-ligand interactions by conducting thermal shift assays (TSA) and analyzed the results with TSAR. We found that the HIV-1 capsid protein hexamers interact with folic acid *in vitro*.

There are reports identifying endogenous metabolites as important cofactors in HIV-1 replication that interact specifically with mature capsid hexamers [47], including IP6 which is found critical for capsid assembly and stability as well as dNTPs that are needed for reverse transcription and genome replication [16-19, 26, 27]. This study does not establish the biological

significance of folic acid for the replication cycle of HIV-1. Of note, many individuals living with HIV-1 have deficiency in folic acid metabolism [48, 49], though it is not clear these findings are related. Folic acid is an important factor required for cell growth and development; folic acid deficiency can lead to neuronal defects and anemia [50, 51]. Thus, it is of interest that this critical cellular metabolite may interact with and stabilize HIV-1 capsid hexamers. The role and relevance of folic acid in HIV-1 biology remains a topic of investigation, but the findings of the screen reported here indicate the ability for assembled hexamers, but not unassembled monomeric capsid, to interact with folic acid.

5.2 Inhibitory Efforts of Gallic Acid

In previous studies, Gallic acid, extracted from herbal medicine, was shown to inhibit HIV-1 [52, 57]. However, the mechanistic properties were not confidently determined. Here, through the screening of a metabolic acid library against protein CA121, we observed interactions between Gallic acid and CA with a thermal shift of 6.23 °C. Subsequent dosage dependence was tested to confirm the strength of the observed shift.

Given the positive result from thermal shift assay, we tested for antiviral effects on reverse transcription with an *in vitro* system and found inhibition during reverse transcription (Figure 12A-C). While, specific molecular-level binding mechanisms are undetermined through the endogenous reverse transcription (ERT) assays, our biology data suggests that Gallic acid may inhibit the HIV-1 replication during the late stage of second strand transfer where the 50% inhibitory concentration (IC₅₀) is 3.64 μM compared to that of the positive control, PF74, 1.32 μM. Following positive results from IC₅₀ experiment data, we proceeded with antiviral inhibition studies of pseudo-typed HIV-1 and found a 50% effective concentration (EC₅₀) of 19.24 μM. In

short, we hypothesize that Gallic acid's interaction with the capsid protein leads to inhibitory effects of HIV-1 replication.

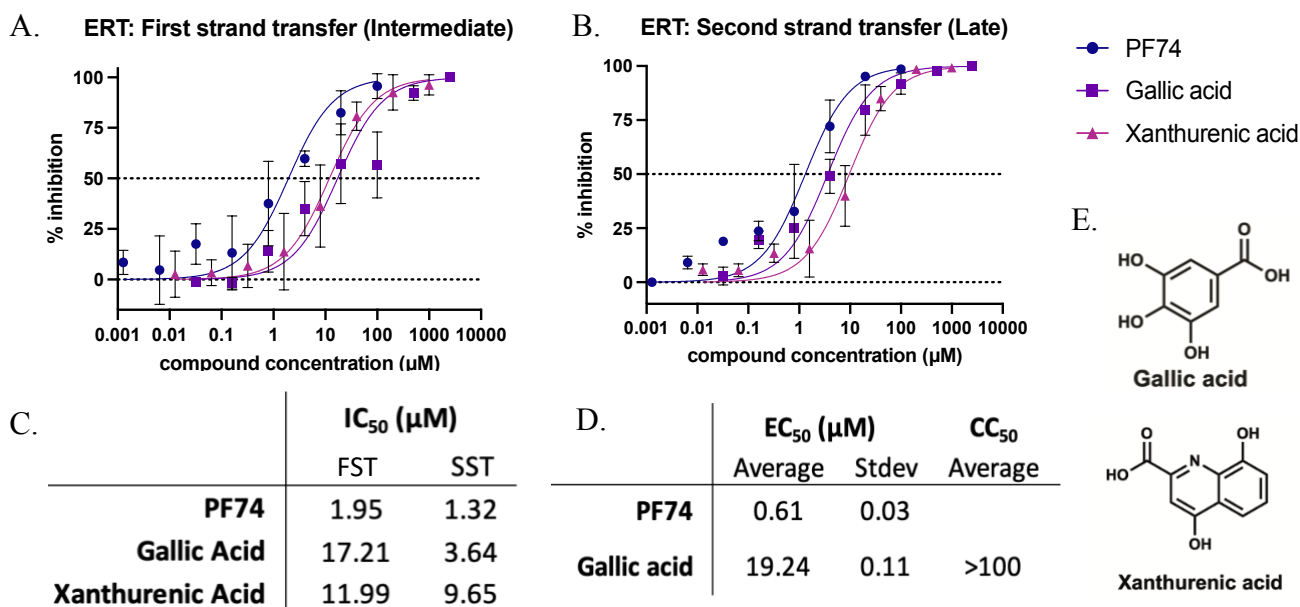


Figure 12. Gallic Acid and Xanthurenic Acid inhibits HIV-1 replication during intermediate and late stages. Using PF74 as positive control, inhibition effects are measured for Gallic Acid and Xanthurenic Acid using Endogenous Reverse-Transcription (ERT) Assay and Antiviral Activity Assay. **a, c)** ERT data showing percent inhibition during the stage of first strand transfer. IC₅₀ concentration numbers are shown in the table under column FSS. Xanthurenic Acid demonstrates more inhibition power during the intermediate stage of HIV replication. **b, c)** ERT data showing percent inhibition during the stage of second strand transfer. IC₅₀ concentration numbers are shown in the table under column SSS. Gallic Acid showcases strong inhibition effect with IC₅₀ SST = 3.64 µM. **d)** Gallic Acid shows inhibition under an EC₅₀ of 19.24 µM without showing cytotoxic effects, CC₅₀ >100. **e)** molecular structure of Gallic acid and Xanthurenic acid generated by chemdraw v 19.0. (Perkin Elmer). A and b were visualized with PRISM V10 (Graphpad).

Endogenous Reverse-Transcription (ERT) Assay presents percent inhibition through the measurement of virion replication at various stages of replication. The assay is performed under series of concentration gradients of ligands, testing HIV-1-like viruses in the cell and monitoring if the virus can successfully produce integrated DNA. PF74 is used as a positive control, known to inhibit reverse transcription of HIV-1 virus. The 50% inhibitory dosage (IC_{50}) of PF74 during the intermediate phase of reverse transcription or First strand transfer (FSS), and the late phase of reverse transcription or second strand transfer (SST) are, 1.95 μM and 1.32 μM respectively. Gallic acid showcases comparatively strong inhibitory effect during SST with an IC_{50} of 3.64 μM , while Xanthurenic acid demonstrates inhibitory effect during both FSS and SST stage with IC_{50} values of 11.99 μM and 9.65 μM . EC_{50} measures the 50% effective concentration where only Gallic acid yielded significant result under 20 μM while having a cytotoxic concentration (CC_{50}) of > 100 μM .

In summary, the data aligns with our hypothesis that there are additional interactions of endogenous metabolites with the HIV-1 capsid proteins. While the interactions leading to inhibition remain unclear, the data presented shed light on the potential roles that host metabolic pathways have during HIV-1 infection and replication.

6. Supplement

6.1 Abbreviations

CA: Capsid Protein

CA FL: Capsid Full-length Protein

TSA: Thermal Shift Assay

TSAR: Thermal Shift Analysis in R

GAM: Generalized Additive Model

ART: Antiretroviral Therapy

ERT: Endogenous Reverse Transcription

IC₅₀: 50% Inhibitory Concentration

EC₅₀: 50% Effective Concentration

CC₅₀: 50% Cytotoxic concentration

a-LA: (±)-α-Lipoic acid

4-ABA: 4-Aminobenzoic acid

B3: Nicotinamide

PyxINE HCl: Pyridoxine hydrochloride

B5: D-Pantothenic acid hemicalcium salt

Thiamin HCl: Thiamine hydrochloride

Pyxal HCl: Pyridoxal hydrochloride

PyxAmine diHCl: Pyridoxamine dihydrochloride

6.2 Supplementary Graphs

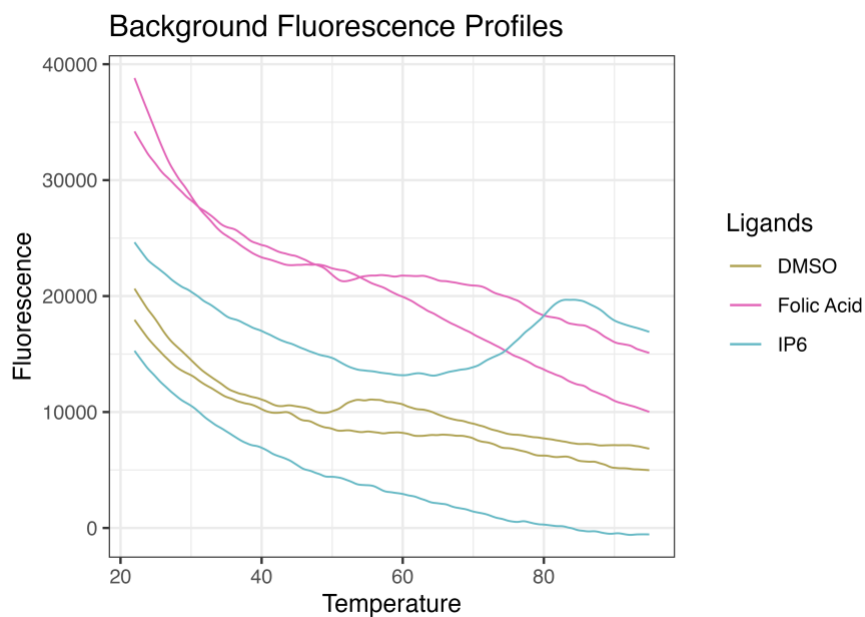


Figure S1. Background Fluorescence Profile of Folic Acid. Experimental setup is similar to a regular TSA protocol with protein CA121 removed. This experiment seeks to eliminate potential background fluorescence from the ligands. Each samples contain DMSO, TRIS buffer, ligand of interest, and fluorescent dye SYPRO™ Orange [4]. No background fluorescence is observed comparing the fluorescence profile of Folic Acid from that of DMSO, negative control.

7. References

1. Andreotti G, Monticelli M, Cubellis MV. Looking for protein stabilizing drugs with thermal shift assay. *Drug Testing and Analysis*. 2015;7(9):831-4. doi: <https://doi.org/10.1002/dta.1798>.
2. Gao K, Oerlemans R, Groves MR. Theory and applications of differential scanning fluorimetry in early-stage drug discovery. *Biophys Rev*. 2020;12(1):85-104. Epub 2020/02/02. doi: 10.1007/s12551-020-00619-2. PubMed PMID: 32006251; PubMed Central PMCID: PMC7040159.
3. Huynh K, Partch CL. Analysis of Protein Stability and Ligand Interactions by Thermal Shift Assay. *Current Protocols in Protein Science*. 2015;79(1):28.9.1-.9.14. doi: <https://doi.org/10.1002/0471140864.ps2809s79>.
4. Magnusson AO, Szekrenyi A, Joosten H-J, Finnigan J, Charnock S, Fessner W-D. nanoDSF as screening tool for enzyme libraries and biotechnology development. *The FEBS Journal*. 2019;286(1):184-204. doi: <https://doi.org/10.1111/febs.14696>.
5. Lo M-C, Aulabaugh A, Jin G, Cowling R, Bard J, Malamas M, et al. Evaluation of fluorescence-based thermal shift assays for hit identification in drug discovery. *Analytical Biochemistry*. 2004;332(1):153-9. doi: <https://doi.org/10.1016/j.ab.2004.04.031>.
6. Niesen FH, Berglund H, Vedadi M. The use of differential scanning fluorimetry to detect ligand interactions that promote protein stability. *Nature Protocols*. 2007;2(9):2212-21. doi: 10.1038/nprot.2007.321.
7. Wu T, Hornsby M, Zhu L, Yu JC, Shokat KM, Gestwicki JE. Protocol for performing and optimizing differential scanning fluorimetry experiments. *STAR protocols*. 2023;4(4):102688.

8. Biter AB, de la Peña AH, Thapar R, Lin JZ, Phillips KJ. DSF Guided Refolding As A Novel Method Of Protein Production. *Scientific Reports*. 2016;6(1):18906. doi: 10.1038/srep18906.
9. Miyazaki Y, Doi N, Koma T, Adachi A, Nomaguchi M. Novel In Vitro Screening System Based on Differential Scanning Fluorimetry to Search for Small Molecules against the Disassembly or Assembly of HIV-1 Capsid Protein. *Front Microbiol*. 2017;8(1413):1413. Epub 2017/08/10. doi: 10.3389/fmicb.2017.01413. PubMed PMID: 28791001; PubMed Central PMCID: PMC5522879.
10. Layton CJ, Hellinga HW. Quantitation of protein–protein interactions by thermal stability shift analysis. *Protein Science*. 2011;20(8):1439-50. doi: <https://doi.org/10.1002/pro.674>.
11. Vernekar SKV, Sahani RL, Casey MC, Kankanala J, Wang L, Kirby KA, et al. Toward Structurally Novel and Metabolically Stable HIV-1 Capsid-Targeting Small Molecules. *Viruses*. 2020;12(4):452. PubMed PMID: doi:10.3390/v12040452.
12. Krishna SN, Luan C-H, Mishra RK, Xu L, Scheidt KA, Anderson WF, et al. A Fluorescence-Based Thermal Shift Assay Identifies Inhibitors of Mitogen Activated Protein Kinase Kinase 4. *PLOS ONE*. 2013;8(12):e81504. doi: 10.1371/journal.pone.0081504.
13. Samuel ELG, Holmes SL, Young DW. Processing binding data using an open-source workflow. *Journal of Cheminformatics*. 2021;13(1):99. doi: 10.1186/s13321-021-00577-1.
14. Chang W, Cheng J, Allaire J, Xie Y, McPherson J, Dipert A, et al. shiny: Web Application Framework for R. 2023.
15. R Core Team. R: A language and environment for statistical computing. 4.3.1 ed. Vienna, Austria: R Foundation for Statistical Computing, ; 2023.

16. Aiken C, Rousso I. The HIV-1 capsid and reverse transcription. *Retrovirology*. 2021;18(1):29. doi: 10.1186/s12977-021-00566-0.
17. Campbell EM, Hope TJ. HIV-1 capsid: the multifaceted key player in HIV-1 infection. *Nat Rev Microbiol*. 2015;13(8):471-83. Epub 2015/07/17. doi: 10.1038/nrmicro3503. PubMed PMID: 26179359; PubMed Central PMCID: PMC4876022.
18. McFadden WM, Snyder AA, Kirby KA, Tedbury PR, Raj M, Wang Z, et al. Rotten to the core: antivirals targeting the HIV-1 capsid core. *Retrovirology*. 2021;18(1):41. doi: 10.1186/s12977-021-00583-z.
19. Müller TG, Zila V, Müller B, Kräusslich H-G. Nuclear Capsid Uncoating and Reverse Transcription of HIV-1. *Annual Review of Virology*. 2022;9(1):261-84. doi: 10.1146/annurev-virology-020922-110929.
20. Dvory-Sobol H, Shaik N, Callebaut C, Rhee MS. Lenacapavir: a first-in-class HIV-1 capsid inhibitor. *Current Opinion in HIV and AIDS*. 2022;17(1):15-21.
21. McFadden WM, Sarafianos SG. Targeting the HIV-1 and HBV Capsids, an EnCore. *Viruses*. 2023;15(4):896. PubMed PMID: doi:10.3390/v15040896.
22. Lamorte L, Titolo S, Lemke CT, Goudreau N, Mercier JF, Wardrop E, et al. Discovery of novel small-molecule HIV-1 replication inhibitors that stabilize capsid complexes. *Antimicrob Agents Chemother*. 2013;57(10):4622-31. Epub 2013/07/03. doi: 10.1128/AAC.00985-13. PubMed PMID: 23817385; PubMed Central PMCID: PMC3811413.
23. Rihn SJ, Wilson SJ, Loman NJ, Alim M, Bakker SE, Bhella D, et al. Extreme Genetic Fragility of the HIV-1 Capsid. *PLOS Pathogens*. 2013;9(6):e1003461. doi: 10.1371/journal.ppat.1003461.

24. Blair WS, Pickford C, Irving SL, Brown DG, Anderson M, Bazin R, et al. HIV capsid is a tractable target for small molecule therapeutic intervention. *PLoS Pathog.* 2010;6(12):e1001220. Epub 2010/12/21. doi: 10.1371/journal.ppat.1001220. PubMed PMID: 21170360; PubMed Central PMCID: PMC3000358.
25. Gres AT, Kirby KA, KewalRamani VN, Tanner JJ, Pornillos O, Sarafianos SG. X-ray crystal structures of native HIV-1 capsid protein reveal conformational variability. *Science.* 2015;349(6243):99-103. Epub 2015/06/06. doi: 10.1126/science.aaa5936. PubMed PMID: 26044298; PubMed Central PMCID: PMC4584149.
26. Jacques DA, McEwan WA, Hilditch L, Price AJ, Towers GJ, James LC. HIV-1 uses dynamic capsid pores to import nucleotides and fuel encapsidated DNA synthesis. *Nature.* 2016;536(7616):349-53. doi: 10.1038/nature19098.
27. Dick RA, Zadrozny KK, Xu C, Schur FKM, Lyddon TD, Ricana CL, et al. Inositol phosphates are assembly co-factors for HIV-1. *Nature.* 2018;560(7719):509-12. doi: 10.1038/s41586-018-0396-4.
28. Renner N, Mallery DL, Faysal KMR, Peng W, Jacques DA, Böcking T, et al. A lysine ring in HIV capsid pores coordinates IP6 to drive mature capsid assembly. *PLOS Pathogens.* 2021;17(2):e1009164. doi: 10.1371/journal.ppat.1009164.
29. Castellano P, Prevedel L, Valdebenito S, Eugenin EA. HIV infection and latency induce a unique metabolic signature in human macrophages. *Scientific Reports.* 2019;9(1):3941. doi: 10.1038/s41598-019-39898-5.
30. Clerc I, Abba Moussa D, Vahlas Z, Tardito S, Oburoglu L, Hope TJ, et al. Entry of glucose- and glutamine-derived carbons into the citric acid cycle supports early steps of HIV-1 infection in CD4 T cells. *Nature Metabolism.* 2019;1(7):717-30. doi: 10.1038/s42255-019-0084-1.

31. Gentleman RC, Carey VJ, Bates DM, Bolstad B, Dettling M, Dudoit S, et al. Bioconductor: open software development for computational biology and bioinformatics. *Genome Biology*. 2004;5(10):R80. doi: 10.1186/gb-2004-5-10-r80.
32. Morgan M, Ramos M. BiocManager: Access the Bioconductor Project Package Repository. p. R package version 1.30.22.
33. Posit team. RStudio: Integrated Development Environment for R. 2023.
34. Wickham H, Hester J, Chang W, J B. devtools: Tools to Make Developing R Packages Easier. 2022.
35. Wickham H, Averick M, Bryan J, Chang W, McGowan LDA, François R, et al. Welcome to the Tidyverse. *Journal of open source software*. 2019;4(43):1686.
36. Ooms J. The jsonlite Package: A Practical and Consistent Mapping Between JSON Data and R Objects. arXiv:1403 2805 [stat CO]. 2014.
37. Schauburger P, Walker A. openxlsx: Read, Write and Edit xlsx Files. 2023.
38. Wood SN. Fast stable restricted maximum likelihood and marginal likelihood estimation of semiparametric generalized linear models. *Journal of the Royal Statistical Society (B)*. 2011;73(1):3-36.
39. Wood SN, Pya N, Saefken B. Smoothing parameter and model selection for general smooth models (with discussion). *Journal of the American Statistical Association*. 2016;111:1548-75.
40. Wood SN. *Generalized Additive Models: An Introduction with R*. 2017. Epub 2.
41. Elzhov TV, Mullen KM, Spiess A-N, Bolker B. minpack.lm: R Interface to the Levenberg-Marquardt Nonlinear Least-Squares Algorithm Found in MINPACK, Plus Support for Bounds. 2023.
42. Perrier V, Meyer F, Granjon D. shinyWidgets: Custom Inputs Widgets for Shiny. 2023.

43. Sievert C. Interactive Web-Based Data Visualization with R, plotly, and shiny. 2020.
44. Attali D. shinyjs: Easily Improve the User Experience of Your Shiny Apps in Seconds. 2021.
45. Owen J. rhandsontable: Interface to the 'Handsontable.js' Library. 2021.
46. Kassambara A. ggpubr: 'ggplot2' Based Publication Ready Plots. R package version 0.6.0 ed2023. p. R package version 0.6.0}.
47. Pornillos O, Ganser-Pornillos BK, Kelly BN, Hua Y, Whitby FG, Stout CD, et al. X-ray structures of the hexameric building block of the HIV capsid. *Cell*. 2009;137(7):1282-92. Epub 2009/06/16. doi: 10.1016/j.cell.2009.04.063. PubMed PMID: 19523676; PubMed Central PMCID: PMCPMC2840706.
48. Adhikari PM, Chowta MN, Ramapuram JT, Rao S, Udupa K, Acharya SD. Prevalence of Vitamin B(12) and folic acid deficiency in HIV-positive patients and its association with neuropsychiatric symptoms and immunological response. *Indian J Sex Transm Dis AIDS*. 2016;37(2):178-84. Epub 2016/11/29. doi: 10.4103/0253-7184.192117. PubMed PMID: 27890954; PubMed Central PMCID: PMCPMC5111305.
49. Revell P, O'Doherty MJ, Tang A, Savidge GF. Folic acid absorption in patients infected with the human immunodeficiency virus. *Journal of Internal Medicine*. 1991;230(3):227-31. doi: <https://doi.org/10.1111/j.1365-2796.1991.tb00435.x>.
50. Donnelly JG. Folic Acid. *Critical Reviews in Clinical Laboratory Sciences*. 2001;38(3):183-223. doi: 10.1080/20014091084209.
51. Mahmood L. The metabolic processes of folic acid and Vitamin B12 deficiency. *Journal of Health Research and Reviews (In Developing Countries)*. 2014;1(1):5-9.

52. Nutan, Sharma, A., Verma, M., Kandwal, M.K., Joshi, V.K., Rishi, P. (2013). Ellagic acid & gallic acid from *Lagerstroemia speciosa* L. inhibit HIV-1 infection through inhibition of HIV-1 protease & reverse transcriptase activity. *The Indian Journal of Medical Research*, 137(3), 540-548.
53. Gao, X., McFadden, W. M., Wen, X., Emanuelli, A., Lorson, Z. C., Zheng, H., Kirby, K. A., & Sarafianos, S. G. (2023). Use of TSAR, Thermal Shift Analysis in R, to identify Folic Acid as a Molecule that Interacts with HIV-1 Capsid. *bioRxiv*. Advance online publication. <https://doi.org/10.1101/2023.11.29.569293>
54. Cercignani, C. (1975). *The Boltzmann Equation and Its Applications*.
55. Christopoulos, Demetris. (2016). On the Efficient Identification of an Inflection Point. *INTERNATIONAL JOURNAL OF MATHEMATICS AND SCIENTIFIC COMPUTING (ISSN: 2231-5330)*. 6.
56. Schroeder, D. V. (2000). *An Introduction to Thermal Physics*.
57. Kahkeshani, N., Farzaei, F., Fotouhi, M., Alavi, S. S., Bahramsoltani, R., Naseri, R., Momtaz, S., Abbasabadi, Z., Rahimi, R., Farzaei, M. H., & Bishayee, A. (2019). Pharmacological effects of gallic acid in health and diseases: A mechanistic review. *Iranian journal of basic medical sciences*, 22(3), 225–237. <https://doi.org/10.22038/ijbms.2019.32806.7897>